

Miniature Trapped-Ion Frequency Standard with $^{171}\text{Yb}^+$

Peter D. D. Schwindt, Yuan-Yu Jau, Heather L. Partner,^{*} Darwin Serkland, Aaron Ison, Andrew McCants, and Edward Winrow
 Sandia National Laboratories
 Albuquerque, NM, USA
 pschwin@sandia.gov

John Prestage, James Kellogg, Nan Yu
 Jet Propulsion Laboratory
 Pasadena, CA, USA

C. Daniel Boschen, Igor Kosvin, David Mailloux, and David Scherer
 Microsemi, Inc.
 Beverly, MA, USA

Craig Nelson, Archita Hati, and David Howe
 National Institutes of Standards and Technology
 Boulder, CO, USA

Abstract—We describe the development and frequency instability measurements of a highly miniaturized, buffer gas cooled, trapped-ion atomic clock. The clock utilizes the 12.6 GHz hyperfine transition of the $^{171}\text{Yb}^+$ ion. A custom-built 3 cm³ vacuum package containing the ion trap is integrated with other key elements of the atomic frequency standard, including a photo multiplier tube, miniaturized laser sources at 369 nm and 935 nm, a local oscillator, and control electronics. With the clock physics package assembled on a 10 cm x 15 cm breadboard, the long-term fractional frequency instability was measured to be 6×10^{-14} at 25 days of integration. Later, the clock physics package was further miniaturized, and the frequency instability was measured to be $2 \times 10^{-11}/\tau^{1/2}$ at integration times up to 10,000 s.

Keywords—atomic clock; trapped ions;

I. INTRODUCTION

Miniature atomic clocks are thought to have a broad range of potential applications including precision navigation, mobile high-speed communications, secure anti-jamming communications, and remote sensing. Vapor-cell based miniature atomic clocks, such as the CSAC (chip-scale atomic clock) [1, 2], have been developed and commercialized over the past decade. Miniature vapor cell clocks, however, suffer from long-term frequency drift mechanisms and therefore can only be used for short-term applications with periodic calibrations. For achieving improved long-term and short-term performance in miniature atomic clocks, ion-trapping technology has several advantages. Because of the robust ion-trapping mechanism (\sim eV trap depth), trapped ions are well

Sandia National Laboratories is a multi-program laboratory managed and operated by Sandia Corporation, a wholly owned subsidiary of Lockheed Martin Corporation, for the U.S. Department of Energy's National Nuclear Security Administration under contract DE-AC04-94AL85000.

This research was developed with funding from the Defense Advanced Research Projects Agency (DARPA). The views, opinions, and/or findings contained in this article are those of the authors and should not be interpreted as representing the official views or policies of the Department of Defense or the U.S. Government. Approved for public release, distribution unlimited.

Some of the measurements presented were made at NIST in Boulder, CO. However, the measurement results are not deemed an endorsement by NIST.

^{*} Present address: Humboldt University of Berlin, Berlin, Germany.

isolated from the environment and insensitive to vibrations and accelerations. The background gas pressure can be as high as 10^{-4} torr, and therefore no active pumps are required to maintain the vacuum. In fact, buffer-gas cooled trapped-ion systems usually use a few micro-torr of buffer gas, such as He or Ne, to maintain the temperature of the trapped ions around 1000 K. This temperature condition is sufficient for making a microwave atomic clock and does not require the complexity of optical cooling. There have been several high-performance microwave ion clocks reported using trapped Hg and Yb ions [3, 4]. Hence, we believe that microwave ion clocks are well suited for miniaturization. In the past few years, we have focused on developing various technologies for a miniature microwave Yb ion frequency standard, including: miniature, sealed ion-trap vacuum packages; miniature, low-power laser sources; low-power ion trapping [5]; a miniature Yb source [6]; integrated optics; and low-power microwave source and control electronics. In this paper, we present two tests of the performance of a 3 cm³ vacuum package with it being used in two different clock implementations.

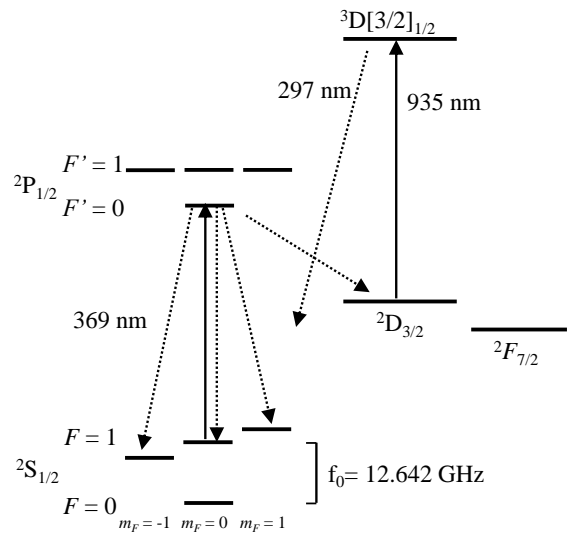


Fig. 1. Partial energy level diagram of $^{171}\text{Yb}^+$.

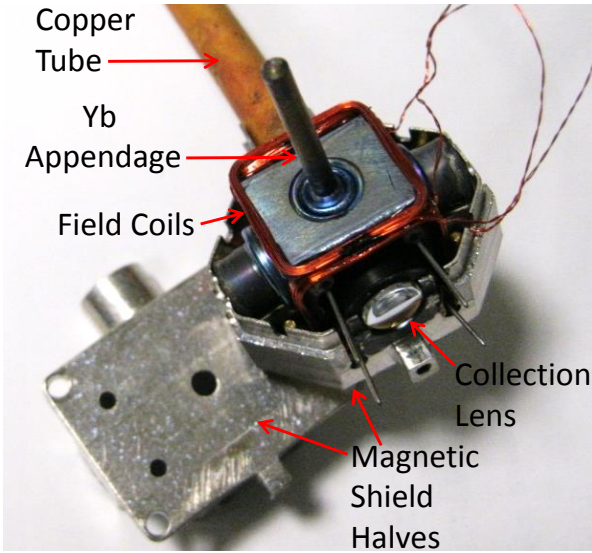


Fig. 2. The vacuum package is pictured while it is nested inside one half of the magnetic shield. The other half of the magnetic shield is below and offset to the left of the vacuum package.

For the miniaturized clock, we chose $^{171}\text{Yb}^+$ for its laser accessible optical transition at 369 nm and its nuclear spin of 1/2. The ground state then contains the $F = 0$ and $F = 1$ hyperfine levels, where the $F = 0$ level contains only a single Zeeman state (Fig. 1), simplifying the optical pumping. At the start of a clock cycle the ions are prepared in the $F = 0$, $m_F = 0$ ground state. A 12.6 GHz microwave field is pulsed on and off to drive a π -pulse from the $F = 0$, $m_F = 0$ state to the $F = 1$, $m_F = 0$ state. To determine how many ions made the transition, the 369 nm and the 935 nm light fields illuminate the ions, and the 297 nm ion fluorescence from the $^3\text{D}[3/2]_{1/2}$ state to the $^2\text{S}_{1/2}$ ground state transition is collected on a detector. The detector signal is conditioned in loop control electronics to generate a control signal to lock the frequency of a local oscillator to the ion hyperfine transition. The state detection process also serves to optically pump the ions back to the $F = 0$ ground state.

II. MINIATURE VACUUM PACKAGE AND ION TRAP

The ^{171}Yb ions are trapped inside of a 3 cm^3 vacuum package (Fig. 2). This package is described in [7], and we provide a short summary here for clarity. The vacuum package is constructed from a titanium body with electrical and optical feedthroughs welded onto the body. The package has three sapphire optical feedthroughs—two are on opposite sides of the package to allow lasers to pass through the center of the ion trap, and the other is used to collect fluorescence from the trapped ions. Titanium tubes are filled with a small amount of Yb metal and welded onto the package to provide a source of neutral Yb for loading the ion trap. There are two Yb oven appendages on opposite sides of the vacuum package, one filled with isotopically purified ^{171}Yb and the other with natural abundance Yb. The ion trap is a linear quadrupole rf Paul trap, and it is positioned in the center of the vacuum package. A copper tube is brazed onto the package to serve as a vacuum pump-out port. Also inside the vacuum package is a non-evaporable getter. Once appropriate vacuum conditions are

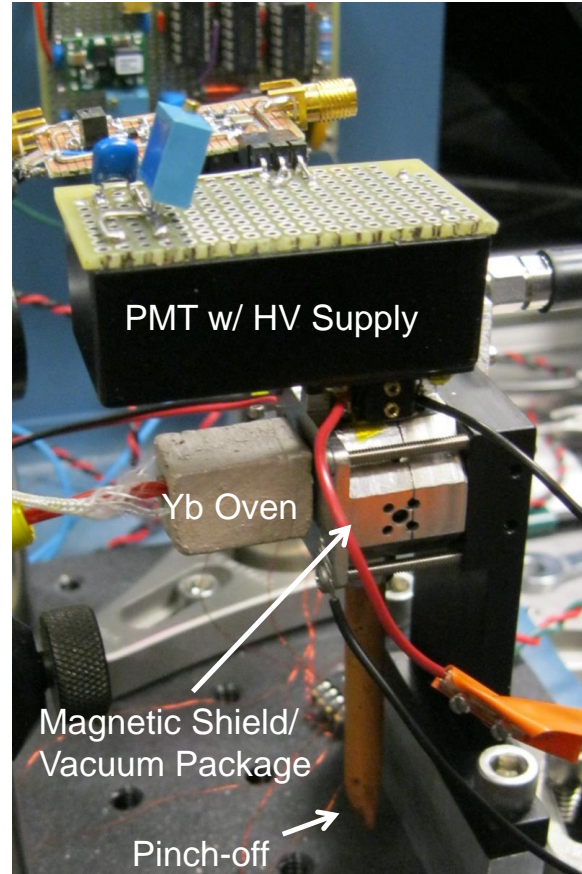


Fig. 3. Photograph of the vacuum package assembled with the PMT and magnetic shield. The vacuum package is pinched off and is pumped only by its internal getter.

achieved through a high temperature bake, the vacuum package is back-filled with 2×10^{-6} torr of helium buffer gas, and the copper tube is pinched off to form a cold weld seal. The process permanently seals the vacuum package, and the getter passively maintains the vacuum.

The vacuum package is assembled with a magnetic shield and photo multiplier tube (PMT) (Fig. 3). A collection lens directs light to the PMT through several fluorescence filters that reject light at the two laser wavelengths of 369 nm and 935 nm but pass the 297 nm fluorescence. Within the magnetic shield is a pair of C-field coils. Around the Yb appendages a small oven is placed to heat the Yb to a temperature of $\sim 450^\circ\text{C}$ to create a vapor of neutral Yb. Ions are created inside the ion trap by illuminating the Yb-coated ion trap electrodes with 405 nm laser light. This creates photoelectrons, which then ionize the Yb through electron impact. The trapping field is created by applying a $190 \text{ V}_{\text{pp}}$ potential difference at 3 MHz to diagonal pairs of the four quadrupole electrodes. A -5 V DC potential applied to the quadrupole trap electrodes relative to the vacuum package walls is maintained to provide the longitudinal confinement of the ions.

III. LONG-TERM FREQUENCY INSTABILITY MEASUREMENTS

For the first clock measurements described in this paper, the vacuum package assembly is mounted on a 10 cm \times 15 cm breadboard. For these first measurements, 20 μ W of 369 nm laser light is brought to the breadboard via an optical fiber. The 369 nm laser source is a large frequency doubled commercial laser system (Toptica TA-SHG pro). The 369 nm light passes through an electrostatically actuated MEMS mechanical shutter. Also mounted on the breadboard is a 935 nm vertical cavity surface emitting laser (VCSEL), and 0.5 mW of this light is combined with the 369 nm light and directed into the vacuum package.

To operate the atomic clock, a custom-built electronics board provides microprocessor control over most functions of the physics package. The electronics board contains a 120-mW oven controlled crystal oscillator (OCXO) (CTS Valpey Corp.) operating at 10 MHz to act as a local oscillator for the clock. (The stability of the OCXO is shown in Fig. 9.) A 12.6 GHz microwave signal, phase locked to the OCXO, drives the hyperfine transition in the $^{171}\text{Yb}^+$ ions. The electronics board also provides current to the 935 nm VCSEL and stabilizes its temperature. The wavelength of the 935 nm VCSEL is stabilized by maximizing the fluorescence signal of the ions. Critical timing control of the clock feedback loop is provided by a field-programmable gate array (FPGA). The FPGA controls the switching of the MEMS shutter and the power from the microwave source. For the data shown in Figs. 4 and 5, the microwave interrogation time is 200 ms while the optical pumping time is 300 ms, such that a single clock cycle has a duration of 500 ms. In between clock cycles, the frequency of the microwave source is hopped to either side of the Yb hyperfine resonance by 4.8 Hz, and the fluorescence signals from every two clock cycles are subtracted to provide feedback to the OCXO. The commercial 369 nm laser is controlled by its own electronics, and its wavelength is locked to a commercial wavemeter.

This breadboard clock system was delivered to the National Institute of Standards and Technology (NIST) for an independent test of its performance. The NIST clock measurement system collected data every 12 minutes. We collected a total of 49 days of good clock data at NIST, and continuous sets of data lasting 6 days, 26 days, 3 days, 4 days, and 10 days were concatenated for Figs. 4 and 5. During this clock test, whenever there was a break in the operation of the clock, ions were reloaded into the ion trap. After the first 6

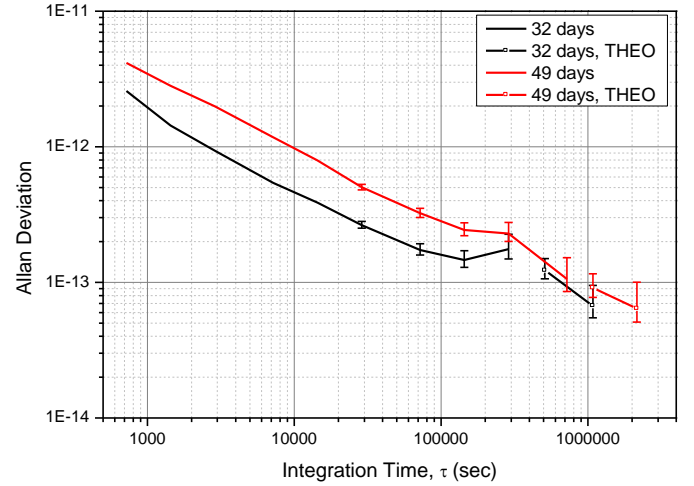


Fig. 4. Allan deviation measurement of the breadboard $^{171}\text{Yb}^+$ clock data. Several phase steps in the data were removed prior to calculating the Allan deviation. The black line shows the Allan deviation for the first 32 days of the composite data set. The last two points of each data set are calculated using the THEO statistic.

days of data collection, the 935 nm VCSEL was replaced because the previous VCSEL was continuously drifting to longer wavelengths and no longer had the ability to be tuned onto the $^2\text{D}_{3/2}$ to $^3\text{D}[3/2]_{1/2}$ optical transition. After the VCSEL was replaced, we achieved continuous autonomous operation of the clock for 31 days. However, the data was broken up due to the 369 nm laser coming unlocked and a four day section where the clock was running at a distinctly different frequency due to excessive 369 nm laser frequency and amplitude noise. During the 31 day run, the ion trap was not reloaded, demonstrating a $1/e$ lifetime of the trapped ions of approximately 3 weeks.

As can be seen in Fig. 5, the short-term stability is degraded after day 32 of the composite data set. After day 32, the new 935 nm VCSEL came out of lock because the laser wavelength drifted to longer wavelengths over time. To bring the laser back on wavelength, the current needed to be reduced, thereby reducing the 935 nm power, resulting in a reduced fluorescence signal from the ions and a degraded short-term stability. However, the long-term stability was not affected, and using the THEO statistic [8], we demonstrated a long-term stability of 6×10^{-14} . The frequency reproducibility between data sets was 2×10^{-13} . With the 49 day measurement, the clock did not reach a flicker floor, pointing to the stability of a trapped ion system utilizing a highly miniaturized package.

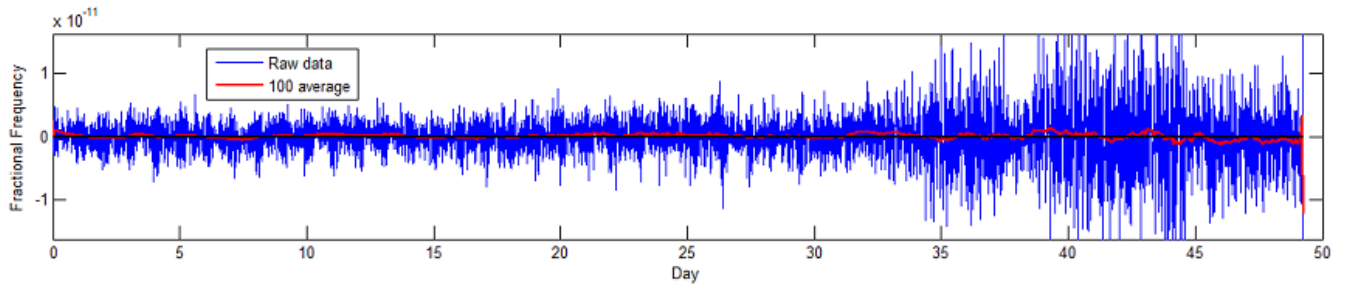


Fig. 5. The fractional frequency deviation is plotted as a function of time for the composite data set. The short-term stability of the clock can be seen to degrade at about day 32. This was due to the reduced power output of the 935 nm laser.

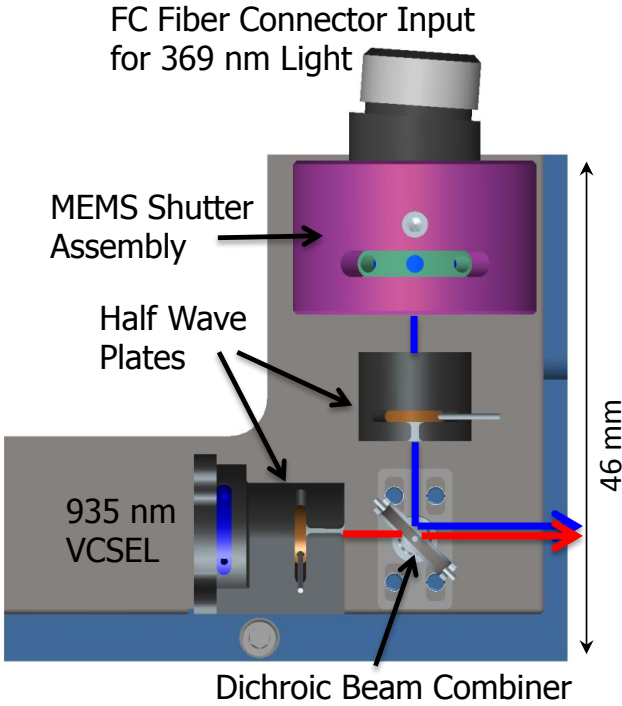


Fig. 6. Schematic of the integrated optical package.

IV. INTEGRATED CLOCK PHYSICS PACKAGE

Subsequent to the measurements at NIST, we developed a much more integrated clock using the same vacuum package assembly that was used for the NIST measurements (and is shown in Figs. 2 and 3). The new system contains an integrated optical package, a miniaturized 369 nm laser, and a physics package interface board. In addition, a new control electronics board was made.

The integrated optical package includes the 935 nm VCSEL and its collimating lens, two half wave plates (one for 935 nm light and the other for 369 nm light), an angle polished FC fiber connector input for the 369 nm light, an assembly to hold the MEMS shutter, and a dichroic beam combiner. The 935 nm VCSEL used in the integrated optical package was newly fabricated and no longer showed the wavelength drift problem observed in the previous measurements. The most complex aspect of the integrated optical package was the MEMS shutter assembly. Since the MEMS shutter moves only 60 μm , the light must pass through a focus to be effectively shuttered by the small shutter blade. In addition, the shutter must be packaged with a 50 μm pinhole to provide an extinction ratio of 40 dB and 94% transmission when open. Alignment of the fiber to the MEMS shutter is achieved by fine positioning of the FC fiber holder. The two waveplates are mounted in holders, which allow adjustment of their angle. Overlap of the 369 nm and 935 nm beams is accomplished by active alignment of the dichroic beam combiner along with an adjustment of the 935 nm VCSEL assembly in and out of the plane of Fig. 6. Through a 5-axis adjustment scheme the two beams are overlapped, and once the correct position for the dichroic beam combiner is established, it is fixed in position with an epoxy.

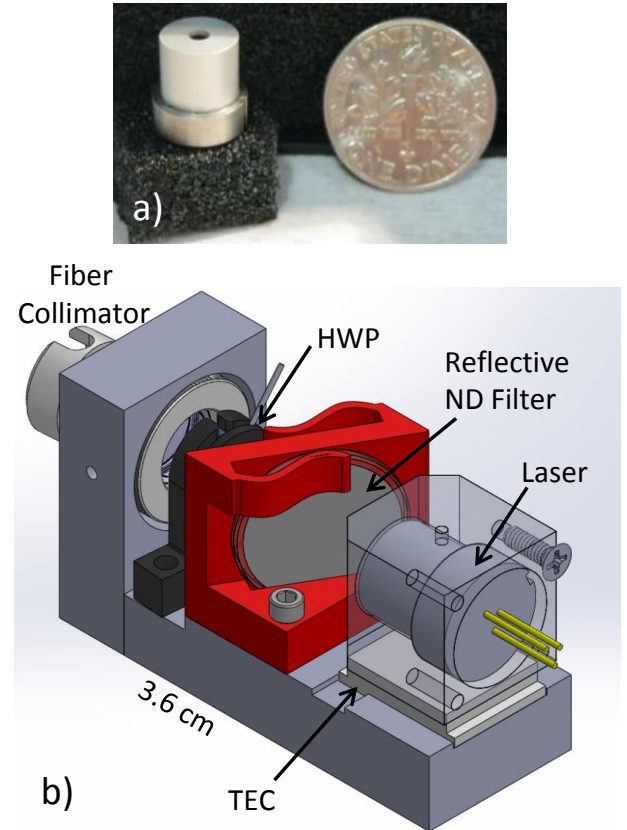


Fig. 7. (a) Photograph of the direct diode 369 nm ECDL with a U.S. dime.
(b) Schematic of the fiber coupling package for the 369 nm laser.

The physics package interface board is designed to be mounted directly on the vacuum package. It provides the required rf trapping voltages [5], current to the C-field coil, and a microwave synthesizer to produce the 12.6 GHz microwave radiation. The synthesizer utilizes the 10 MHz signal from the OCXO on the control electronics board.

The miniaturized 369 nm laser is a direct diode source. An external cavity diode laser (ECDL) is made using a diode laser from Nichia Corp. that is selected with a wavelength of < 371

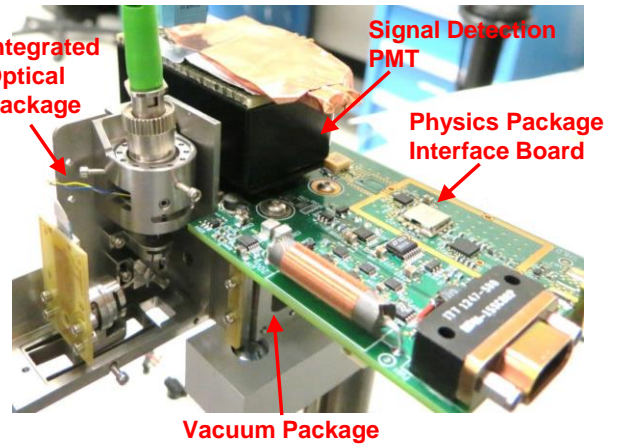


Fig. 8. Integrated physics package including the optical package and the physics package interface board.

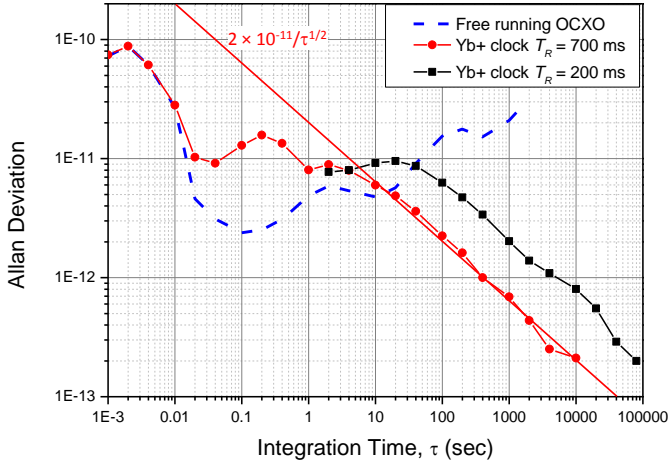


Fig. 9. Allan deviation of the integrated clock. T_R is the microwave interrogation time. The red line is a guide to the eye showing $2 \times 10^{-11}/\tau^{1/2}$ performance.

nm. Then, the laser is packaged by Ondax, Inc. with a collimating lens and a volume holographic grating, forming the ECDL (Fig. 7(a)). The packaged size of the laser is $\sim 1 \text{ cm}^3$. This laser is mounted in a custom-built fiber coupling package to deliver light to the integrated optical package (Fig. 7(b)). The fiber coupling package is 10 cm^3 in size.

With the Ondax packaging, the laser wavelength is tuned with current and temperature—there is no direct control of the cavity length. By tuning the wavelength of the laser with current, we can achieve a mode-hop-free-tuning range of 8 GHz. As is typical with ECDLs, the laser has several modes that it hops through as the current is tuned, but the exact wavelength range of continuous tuning within a mode varies with temperature. This laser is quite stable over a time scale of several hours. However, over days and weeks the wavelengths of the modes drift, and new temperature and current settings need to be found so that the laser operates at the 369 nm optical transition. Long-term measurements indicate that to operate at the required wavelength, one must slowly increase the laser temperature over time. Because of the slowly drifting mode structure, the longest we could ever run the clock without the laser mode-hopping was 7 days. When the laser mode-hops, we need to stop clock operation for several hours while new laser operating parameters are found.

While operating the clock, both the 369 nm and 935 nm lasers need to be stabilized. Instead of using commercial wavemeters for laser frequency stabilization, we have utilized temperature-stabilized, miniature etalons ($6 \times 6 \times 12 \text{ mm}^3$) for short-term (up to several hours) laser frequency stabilization. The long-term laser stability can be in-principle maintained by servoing the etalon temperatures and using the ion signal to maximize the fluorescence. We have demonstrated locking of both the 369 nm and 935 nm lasers to etalons. In fact, for the data shown in Fig. 9, the 935 nm laser is locked to an etalon. The 369 nm laser was still stabilized by a wavemeter due to a minor technical conflict that prevents us from locking the 369 nm laser while recording the clock data.

The changes to the updated control electronics board most pertinent to the data shown in Fig. 9 were changes to both the

hardware and firmware that allowed an increase in the total time of the clock cycle and an increased frequency resolution in the microwave synthesizer. The previous board allowed only a 655 ms clock cycle and a minimum frequency step of 1.6 Hz for the 12.6 GHz microwave synthesizer. In this new board, a clock cycle time of 20 s and a minimum microwave frequency step of 0.1 Hz are possible. Longer interrogation time allows us to take advantage of the coherence time of the trapped ions. In our case, the limiting factor is the low-power OCXO. We found the optimal clock cycle time was 1 s with 700 ms of microwave interrogation and 300 ms of optical pumping. At microwave interrogation times longer than 700 ms, the instability of the OCXO would broaden the linewidth of the Yb hyperfine transition. Fig. 9 shows the advantage of going from a 200 ms microwave interrogation time to 700 ms. To truly take advantage of the long coherence time of the buffer-gas-cooled trapped ions, an improved local oscillator is needed.

V. CONCLUSION

To our knowledge, this is the smallest trapped-ion frequency standard published to date. The volume of all of the components of the physics package including the etalons for laser lock is $\sim 100 \text{ cm}^3$, and the power consumption of the clock is $< 1 \text{ W}$. The titanium vacuum package technology has proven to be very robust. At the time of measurements of Fig. 9 the vacuum package had been sealed and passively pumped by the getter for two years. Since the first two months after sealing the vacuum package, we have seen no significant changes in the trapped ion lifetime and the number of trapped ions after reloading the trap.

An area of significant potential improvement is in the fluorescence signal size from the trapped ions. For the data in Fig. 9, the clock is operating at the photon shot noise limit. During operation of the clock, we observe that 70-80% of the ions are in the long-lived $^2F_{7/2}$ -state and are not contributing to the fluorescence signal. While the clock still operates well, it would be advantageous to eliminate this significant F -state trapping. A laser could be used to move population out of the F -state, but this approach is not desirable for a small, low-power atomic clock. Additionally, nitrogen buffer gas has been shown to quench the F -state [9]. However, nitrogen is pumped by the getter in the vacuum package. It may be possible to use a hydrocarbon buffer gas since it is not pumped by the getter, and we have initial results indicating that methane may work well to quench the F -state. Signal improvements may also be achieved by collecting fluorescence at 369 nm. There are 200 times more photons per ion emitted at 369 nm compared to 297 nm. Thus far, we have achieved the best signal to noise ratio by collecting 297 nm fluorescence because of the high scattered light background from the 369 nm laser. We believe that in the miniaturized physics package, with careful control of the 369 nm light scatter, detection at 369 nm is possible, which would greatly enhance the signal size.

While we have achieved a great deal of miniaturization, additional improvements in the component technologies of the clock could lead to perhaps another factor of ten reduction in the size of the clock. We have already demonstrated a vacuum package with a volume $< 1 \text{ cm}^3$, and this result is to be reported in a later publication. The component that requires the most

development at this point is the 369 nm laser. The current direct diode source consumes several hundred milliwatts of power and has poor long-term stability. Improvements in the 369 nm laser technology would enable a new class of low-power, long-term stable trapped-ion atomic clock. Overall the ^{171}Yb ion clock shows excellent stability in a small package and shows promise as a highly miniaturized frequency standard.

REFERENCES

- [1] S. Knappe, et al., "A microfabricated atomic clock," *Applied Physics Letters*, vol. 85, pp. 1460-1462, Aug 30 2004.
- [2] R. Lutwak, et al., *The miniature atomic clock - Pre-production results*. New York: IEEE, Electron Devices Soc & Reliability Group, 2007.
- [3] J. D. Prestage and G. L. Weaver, "Atomic clocks and oscillators for deep-space navigation and radio science," *Proceedings of the Ieee*, vol. 95, pp. 2235-2247, Nov 2007.
- [4] P. T. H. Fisk, et al., "Accurate measurement of the 12.6 GHz "clock" transition in trapped $\text{Yb-171}(+)$ ions," *Ieee Transactions on Ultrasonics Ferroelectrics and Frequency Control*, vol. 44, pp. 344-354, Mar 1997.
- [5] Y. Y. Jau, et al., "Low power high-performance radio frequency oscillator for driving ion traps," *Review of Scientific Instruments*, vol. 82, Feb 2011.
- [6] R. P. Manginell, et al., "In situ dissolution or deposition of Ytterbium (Yb) metal in microhotplate wells for a miniaturized atomic clock," *Optics Express*, vol. 20, pp. 24650-24663, Oct 22 2012.
- [7] Y. Y. Jau, et al., "Low-power, miniature Yb-171 ion clock using an ultra-small vacuum package," *Applied Physics Letters*, vol. 101, Dec 17 2012.
- [8] T. N. Tasset, et al., "Theo1 confidence intervals frequency stability measurement applications," *Proceedings of the 2004 IEEE International Frequency Control Symposium And Exhibition (IEEE Cat. No.04CH37553C)*, pp. 725-728, 2004 2004.
- [9] D. J. Seidel and L. Maleki, "Efficient quenching of population trapping in excited Yb^+ ," *Physical Review A (Atomic, Molecular, and Optical Physics)*, vol. 51, pp. R2699-R2702, April 1995.